Published in final edited form as:
Cell Metab. 2011 June 8; 13(6): 655–667. doi:10.1016/j.cmet.2011.03.023.

Autophagy Regulates Cholesterol Efflux from Macrophage Foam Cells via Lysosomal Acid Lipase

Mireille Ouimet[1], **Vivian Franklin**[1], **Esther Mak**[1], **Xianghai Liao**[2], **Ira Tabas**[2,3,4], and **Yves L. Marcel**[1,*]

[1]University of Ottawa Heart Institute, Ottawa, ON K1Y 4W7, Canada

[2]Department of Medicine, Columbia University, New York, NY 10032, USA

[3]Department of Pathology and Cell Biology, Columbia University, New York, NY 10032, USA

[4]Department of Physiology and Cellular Biophysics, Columbia University, New York, NY 10032, USA

SUMMARY

The lipid droplet (LD) is the major site of cholesterol storage in macrophage foam cells and is a potential therapeutic target for the treatment of atherosclerosis. Cholesterol, stored as cholesteryl esters (CEs), is liberated from this organelle and delivered to cholesterol acceptors. The current paradigm attributes all cytoplasmic CE hydrolysis to the action of neutral CE hydrolases. Here, we demonstrate an important role for lysosomes in LD CE hydrolysis in cholesterol-loaded macrophages, in addition to that mediated by neutral hydrolases. Furthermore, we demonstrate that LDs are delivered to lysosomes via autophagy, where lysosomal acid lipase (LAL) acts to hydrolyze LD CE to generate free cholesterol mainly for ABCA1-dependent efflux; this process is specifically induced upon macrophage cholesterol loading. We conclude that, in macrophage foam cells, lysosomal hydrolysis contributes to the mobilization of LD-associated cholesterol for reverse cholesterol transport.

INTRODUCTION

Macrophage foam cells are a key component of atherosclerotic lesions. Because enhancing cholesterol efflux from these cells is an attractive means to reverse plaque lipid buildup, there has been continued investigation on ways to promote net cholesterol flux from peripheral tissues to the liver for excretion via the bile, a process referred to as macrophage reverse cholesterol transport (RCT) (Khera and Rader, 2010). The first step in RCT is the release of cholesterol from lipid droplets (LDs). Although classically defined as the cellular cholesterol “storage” organelle, current research highlights the dynamic nature of LDs (Farese and Walther, 2009). LDs are comprised of a neutral lipid core delineated by a phospholipid monolayer, which is coated by proteins. Adipophilin is the macrophage LD coat protein, and its levels are directly correlated to cellular neutral lipid content and, recently, to atherosclerosis (Paul et al., 2008). It is important to understand how cholesteryl esters (CEs) in LDs are hydrolyzed and mobilized for efflux, given that cytoplasmic CE

*Correspondence: ylmarcel@ottawaheart.ca.

SUPPLEMENTAL INFORMATION

The Supplemental Information includes three figures, two movies, Supplemental Experimental Procedures, and Supplemental References and can be found with this article online at doi:10.1016/j.cmet.2011.03.023.

hydrolysis is increasingly becoming recognized as the rate-limiting step for cholesterol efflux and whole-body RCT (Ghosh et al., 2010).

Macroautophagy (hereafter referred to as autophagy) has been shown to participate in glucose, protein, and, recently, lipid metabolism (Kovsan et al., 2009). The autophagic process involves the formation of double membrane autophagosomes that sequester cytoplasmic contents and subsequently fuse with lysosomes, thus delivering the autophagic body into the lysosomal lumen for degradation (Klionsky, 2005). The initiating event in autophagy is nucleation of the membrane that will form the autophagosome (Tooze and Yoshimori, 2010), after which the microtubule-associated protein 1A/1B light chain 3 (LC3) conjugation system acts in membrane elongation and autophagosome formation (Tanida, 2010). Following autophagosome fusion with the lysosome, cytosolic components sequestered in the autophagosome are degraded by acid proteases and hydrolases in the autolysosome.

The idea that autophagy is simply a means for bulk degradation of cytoplasmic constituents is changing as examples of preferential targeting of cargo for autophagic degradation emerge, revealing the selectivity of the process (Weidberg et al., 2009). In addition to the forms of selective autophagy previously described, such as xenophagy (selective delivery of microorganisms to lysosomes), pexophagy (selective peroxisome cargo), mitophagy, ribophagy, ERphagy, etc., each of which possesses unique protein requirements (Weidberg et al., 2009), a type of autophagy describing the selective delivery of LDs for lysosomal degradation was recently described and has been termed “lipophagy” (Singh et al., 2009a). Here, we report that in atherogenic pathophysiological conditions (exposure to modified low-density lipoprotein [LDL]), autophagy is activated in macrophages, and this process contributes to intracellular lipid breakdown. Cytoplasmic LD-associated CE delivered to lysosomes by way of autophagy undergoes lysosomal acid lipase (LAL)-dependent lipolysis, thereby generating free cholesterol for efflux to a cholesterol acceptor. Consequently, cholesterol efflux from lipid-loaded macrophages is dependent upon LD catabolism by autophagy, and the importance of this process in whole-body RCT is highlighted by the impaired ability of *Atg5*$^{-/-}$ macrophages to clear accumulated ^{3}H-cholesterol in vivo.

RESULTS

Lysosomes Contribute to Lipid Breakdown in Macrophage Foam Cells

Because the internalization of modified LDL is an unregulated process that leads to foam cell formation (Goldstein et al., 1979; Shashkin et al., 2005), we used acetylated LDL (AcLDL) to elevate macrophage intracellular cholesterol levels. Bone marrow-derived macrophages were incubated with AcLDL for 30 hr, after which the cells were washed and the lipoproteins were chased during an overnight equilibration. At this time, all of the AcLDL was degraded and excess cholesterol was stored as neutral lipids in cytoplasmic LDs (see Figure S1 available online). Whereas oxidized LDL (OxLDL) tends to become trapped within the endolysosomal compartment (Schmitz and Grandl, 2009), AcLDL is known to be quite rapidly processed in the lysosome, and the majority of its associated cholesterol is stored in cytoplasmic LDs (Brown et al., 1979; Cox et al., 2007; Itabe et al., 2000; Jerome et al., 1998; Yancey and Jerome, 1998). Bodipy 493/503 is commonly used to fluorescently stain neutral lipids (Listenberger and Brown, 2007). To visualize LDs in real time, neutral lipids were stained with Bodipy and the cells were observed by confocal microscopy in a 37°C heat chamber. Macrophage LDs could be seen surrounding an unidentified circular organelle, and over time the formation of a “ring” stained for neutral lipids could be observed around this unknown organelle (Figure 1A and Movie S1).

Recently, it was suggested that LDs could undergo transient heterotypic fusion events with bilayered organelles, whereby lipids transferred from the LDs to the space between the leaflets of the phospholipid bilayer surrounding the recipient organelle could subsequently be hydrolyzed and incorporated into the recipient organelle (Murphy et al., 2008). To investigate whether such an event was occurring in our cells, LDs were observed in the presence of LysoTracker Red, which stains acidic organelles. Interestingly, the neutral lipid rings that seem to originate from LDs overlapped with acidic rings (arrows, Figure 1B and Movie S2), and even more intriguing, some LDs were entirely surrounded by acidic rings (asterisks, Figure 1B), suggesting that they had fused with acidic organelles. To determine whether the acidic organelle within which LDs could be observed was the lysosome, we incubated the cells with DQ Red BSA, which selectively fluoresces in the degradative environment of the lysosome. Indeed, LDs were observed within lysosomes (arrowheads, Figure 1C). The proportion of LD neutral lipids within lysosomes was 15% ± 5%. Because of the colocalization between the macrophage LD coat protein adipophilin and lysosomal-associated membrane protein 1 (LAMP-1)-positive lysosomes (Figure 1D), we concluded that the neutral lipid observed within lysosomes was LD-associated CE, and not simply CE from undigested AcLDL. The frequency at which adipophilin was found within lysosomes (9% ± 3%) was similar although slightly lower than that observed for neutral lipids. Together, these observations led us to postulate that lysosomes may contribute to LD-associated CE hydrolysis in macrophage foam cells.

While the importance of mobilizing cholesterol from LDs is acknowledged, it remains a poorly understood process. Many candidate neutral CE hydrolases have been identified, none of which has been unambiguously shown to be responsible for all CE hydrolytic activity in macrophages; individual contributions of the various CE hydrolases have yet to be defined (Ghosh et al., 2010). Paraoxon or E600, which binds irreversibly to the active site of lipases such as carboxylesterases (Ileperuma et al., 2007), is commonly used as a general lipase inhibitor (Wei et al., 2007). To determine the importance of neutral and potentially acid hydrolases in macrophage CE hydrolysis, we added paraoxon (to inhibit neutral CE hydrolysis) or chloroquine, a lysosomotropic agent that interferes with vesicular acidification (to inhibit lysosomal CE hydrolysis), during incubation of lipid-loaded macrophages with lipid-poor apoA-I. Because macrophage CE undergoes a continual cycle of hydrolysis and re-esterification (Brown et al., 1980), we included an ACAT inhibitor during this period to prevent the re-esterification of hydrolyzed CE. We found that macrophage CE mass increased in both chloroquine- and paraoxon-treated cells, their compound effect being cumulative (Figure 1E). The independent inhibition of neutral and lysosomal CE hydrolysis resulted in a substantial decrease in CE hydrolysis, whereas inhibition of both pathways abolished CE hydrolysis entirely (Figure 1F).

To evaluate whether lysosomal LD-associated CE hydrolysis is implicated in mobilization of cholesterol for efflux, macrophages were loaded with AcLDL containing ^{3}H-cholesterol, and efflux of the labeled cholesterol to lipid-poor apoA-I was measured. AcLDL-derived ^{3}H-cholesterol is esterified in the ER and accumulates in LDs (Figure S1). The movement of ^{3}H-cholesterol from lipid-loaded macrophages to apoA-I is unidirectional and is an accurate parameter of the flux of cholesterol mass out of the cell (Figure S1 and Sankaranarayanan et al., 2010). Paraoxon diminished but did not abolish cholesterol efflux (Figure 1G), implying that an additional mechanism for cholesterol mobilization for efflux in lipid-loaded macrophages exists. In agreement with a role for lysosomal hydrolysis in regulating cytoplasmic CE, the addition of chloroquine also resulted in decreased cholesterol efflux (Figure 1G). Together, these results point to a role for both neutral and acidic CE hydrolysis in mobilizing cholesterol from cytoplasmic CE stores.

Autophagic Flux Modulates Foam Cell Lipolysis

Having established a role for lysosomal function in LD CE hydrolysis and efflux, how LDs became localized within lysosomes was an enigma, particularly since complete fusion between monolayered and bilayered organelles is not possible. A timely report by Singh and colleagues (Singh et al., 2009a), documenting the sequestration of LDs by the autophagic machinery and their subsequent delivery to lysosomes in triglyceride-enriched hepatocytes, provided a plausible explanation for our own observations in CE-enriched macrophages. To assess whether autophagy was involved in LD CE processing in macrophage foam cells, we first searched for evidence of autophagic vacuoles in lipid-loaded macrophages and, if present, whether these were associated with LDs.

The LC3 conjugation system is essential for autophagy (Tanida, 2010). Cytosolic LC3 (LC3-I) is modified to its membrane-bound form (LC3-II), which is located on preautophagosomes and autophagosomes and thus commonly used as an autophagosomal marker (Kabeya et al., 2000). A direct association between LDs and LC3 was observed by immunofluorescence (arrows, Figure 2A). In some instances, multiple LC3 puncta were observed on Bodipy-positive structures larger that the LDs (boxed, Figure 2A) that could represent lysosomes or multivesicular bodies containing significant amounts of neutral lipids (perhaps multiple LDs). Previously described morphological criteria (Singh et al., 2009a) were used to further define LD sequestration by autophagic vesicles by electron microscopy. LDs (stars, Figure 2B) were easily recognized as circular electron-transparent organelles that were not surrounded by the double membrane characteristic of other organelles. Electron microscopy of lipid-loaded macrophages revealed double-membrane vesicles analogous to autophagosomes in and around LDs (arrows, Figure 2B) and degradative structures enriched in LDs (asterisks, Figure 2B). The autophagosomal nature of the double membrane vesicles at the LD periphery was confirmed by LC3 immunogold label (open arrowheads, Figure 2B). Blind counts revealed that 40% of LDs were associated with LC3 (Figure 2F).

Another line of evidence for the association of autophagosomes and LDs was the occurrence of LC3-II protein in the LD fractions of foam cells (Figure 2C). Chloroquine treatment inhibits LC3 degradation, and thus there was increased LC3-II in both the cytoplasmic and LD pools—best seen in 2 and 7 s exposures, respectively. Finally, we evaluated whether a pharmacological modulator of autophagy alters cholesterol efflux. Vinblastine, which inhibits the fusion between autophagosomes and lysosomes, leads to the accumulation of autophagosomes and their associated protein marker, LC3-II (Figure 2D). Inhibition of autophagy by vinblastine in lipid-loaded macrophages reduced cholesterol efflux (Figure 2E). Collectively, these results support a role for autophagy in the degradation of cytoplasmic LDs.

Activation of the Autophagic Machinery in Response to Lipid Loading

Because all cytoplasmic CE hydrolysis has previously been attributed to the action of extralysosomal, neutral CE hydrolases (Brown et al., 1980; Cheng et al., 2006), we were compelled to investigate whether the autophagy-dependent mobilization of cholesterol for efflux observed in our foam cell model was specific to lipid-loaded cells and sensitive to the length of treatment. We found chloroquine to be effective in the attenuation of cholesterol efflux from lipid-loaded cells, but not in LDL-treated, unloaded macrophages (Figure 3A). Chloroquine treatment had no significant effect on AcLDL-loaded cells when included during a 4 hr cholesterol efflux experiment, as previously reported (Brown et al., 1980), but a significant inhibition could be seen at 18 hr (Figure 3B). Thus, lysosomal cytosolic CE hydrolysis is required for cholesterol efflux in lipid-loaded cells; LD-associated CE hydrolysis in macrophage foam cells is not exclusively dependent upon neutral CE hydrolases.

To investigate whether autophagy is specifically induced in macrophage foam cells, we probed protein samples for LC3 and found LC3-II to be elevated in response to lipid loading (Figure 3C). To ensure that the rise in LC3-II was not simply due to defective autophagosome clearance resulting in cellular autophagosome accumulation, chloroquine was added to the media 2 hr prior to protein isolation. A further increase in LC3-II protein upon lysosomal inhibition was observed, indicative of a functional autophagic flux in these cells, as cellular LC3 levels per se are not a good marker for autophagy (Tanida et al., 2005). Thus, autophagy is expressly triggered in macrophages in response to an expanded cytoplasmic cholesterol pool.

LAL is the enzyme that hydrolyzes neutral lipids delivered to lysosomes by receptor-mediated endocytosis (Goldstein et al., 1975). Because the lysosome population within a cell is comprised of a heterogeneous pool of lysosomal subgroups with distinct roles in autophagy (Cuervo et al., 1997), and since it has been proposed that autophagy-competent lysosomes could utilize Atg15, an Atg (autophagy-related gene) family member predicted to hydrolyze neutral lipids (Kovsan et al., 2009), we next sought to determine which acid lipase is implicated in autophagy-mediated LD CE hydrolysis. We used a potent and specific LAL inhibitor, compound 13 or 3a2 (Rosenbaum et al., 2009, 2010), herein referred to as Lalistat 1, to determine whether LAL is implicated in LD breakdown in our foam cell model. As previously shown (Rosenbaum et al., 2009), the administration of Lalistat 1 during AcLDL loading prevents LD formation because Lalistat 1 effectively blocks LAL-mediated AcLDL lipid hydrolysis (Figure S2).

The addition of Lalistat 1 to lipid-loaded cells during cholesterol efflux reduced efflux and resulted in a concomitant rise in cellular CE mass (Figures 3D and 3E). To ensure that the Lalistat 1-inhibitable efflux from AcLDL-loaded macrophages indeed represents LD-associated cholesterol, and not cholesterol associated with AcLDL trapped in lysosomes, we used an ACAT inhibitor to prevent LD formation and measured efflux in the presence of Lalistat 1. We found that in the absence of LDs, inhibition of LAL had no effect on cholesterol efflux, indicating that the Lalistat 1-inhibitable efflux in AcLDL-loaded macrophages is LD cholesterol (Figure S2). Together, these data indicate that autophagy is selectively induced in lipid-loaded cells and mediates the delivery of cytoplasmic LDs to lysosomes, where LD-associated CE is hydrolyzed by LAL to liberate cholesterol for efflux.

Impaired LD Catabolism in *Atg5*$^{-/-}$ Macrophage Foam Cells

Next, we sought to measure cholesterol efflux in macrophages isolated from *Atg5*$^{-/-}$ mice as compared to wild-type (WT) controls. In cells lacking Atg5, the modification of LC3-I to LC3-II is impaired (Mizushima et al., 2001)—corroborated here by the complete absence of LC3-II in these cells (Figure 4A)—and autophagy cannot ensue. Again, autophagosome formation was induced in macrophages in response to lipid loading (Figure 4). Autophagosomes are initiated by repression of the mammalian target of rapamycin (mTOR) or by the class III phosphoinositide 3-kinase (PI3K)/Beclin-1 complex. We have thus far failed to observe changes in Beclin-1 protein levels in lipid-loaded macrophages (Figure 4A), making mTOR a likely candidate for modulating autophagy in foam cells, although an alternative pathway independent of mTOR and class III PI3K/Beclin-1 for triggering of autophagy has also been described (Lepine et al., 2010).

Given that autophagy is required for LD genesis and lipid storage in adipose tissue (Baerga et al., 2009; Singh et al., 2009b; Zhang et al., 2009), along with additional findings that the Atg conjugation system is involved in LD formation in hepatocytes and cardiomyocytes (Shibata et al., 2009), we assessed the ability of autophagy-defective macrophages to accumulate neutral lipids in LDs when exposed to AcLDL. Neutral lipids in AcLDL-loaded *Atg5*$^{-/-}$ macrophages effectively accumulated in LDs, since all cytoplasmic lipid inclusions

were surrounded by adipophilin (Figure 4F, after cholesterol loading). Thus, LD formation in lipid-loaded *Atg5*$^{-/-}$ macrophages occurs normally. Moreover, the extent of cholesterol loading was comparable in WT and *Atg5*$^{-/-}$ macrophages (Figures 4B and 4C). Importantly, cholesterol efflux from lipid-loaded *Atg5*$^{-/-}$ macrophages was significantly reduced as compared to WT macrophages (Figure 4D), likely due to decreased CE hydrolysis in *Atg5*$^{-/-}$ macrophages as compared to WT (Figure 4E).

Our hypothesis that autophagy plays a key role in the efflux of LD cholesterol was further corroborated by microscopic observations showing that accumulated cytoplasmic LDs dissipate after incubation with apoA-I in WT, but not in *Atg5*$^{-/-}$ macrophages (Figure 4F). Adipophilin, whose levels are directly correlated to cellular LD content, also visibly dissipates in WT cells after efflux, but not in *Atg5*$^{-/-}$ cells. The observation that Lalistat 1 treatment impairs cholesterol efflux to apoA-I in WT, but not *Atg5*$^{-/-}$ macrophages (Figure 4D), firmly establishes that autophagy is the means by which LDs are delivered to LAL for hydrolysis. The observation that paraoxon is effective at reducing efflux in both WT and *Atg5*$^{-/-}$ macrophages substantiates the idea that CE hydrolysis by neutral CE hydrolases and autophagy are mutually exclusive pathways. Notably, inhibition of both pathways nearly abolishes all efflux to apoA-I.

To rule out the possibility that the CE accumulation observed in *Atg5*$^{-/-}$ macrophages is due to enhanced esterification of cholesterol or decreased lysosomal hydrolysis of lipoprotein CE in *Atg5*$^{-/-}$ cells compared to WT, we directly measured both of these parameters in WT and *Atg5*$^{-/-}$ macrophages. We found that esterification of lipoprotein ^{3}H-cholesterol to ^{14}C-oleic acid did not differ between WT and *Atg5*$^{-/-}$ macrophages (Figure 4G). Consistent with the well-established role for ACAT in mediating cholesterol esterification in the ER, the esterification of both radiolabels was abolished in the presence of the ACAT inhibitor. Degradation of lipoprotein-associated ^{3}H-cholesteryl oleate was equivalent in WT and *Atg5*$^{-/-}$ macrophages (Figure 4H), indicating that the observed decrease in cholesterol efflux from *Atg5*$^{-/-}$ cells does not result from augmented lipoprotein CE retention in *Atg5*$^{-/-}$ cells as compared to WT. Most importantly, these results clearly demonstrate that AcLDL CE is processed very rapidly in lysosomes as compared to OxLDL CE. During this experiment, only 10% of AcLDL CE remained after a 30 hr incubation. This small amount of residual AcLDL CE minimally decreased during an O/N chase (to 7%–8%) and is likely to represent a background amount that could not account for the relative decrease in cholesterol efflux observed in *Atg5*$^{-/-}$ cells.

Autophagy Is Induced by Atherogenic Lipoproteins and by Cholesterol Loading In Vivo

To further characterize the physiological relevance of this pathway, we tested whether autophagy was also induced in macrophages incubated with pathophysiological forms of modified LDL, such as OxLDL and aggregated LDL (AgLDL), and with very low density lipoprotein (VLDL). We found that, similarly to AcLDL, incubation of macrophages with AgLDL or VLDL resulted in the accumulation of cytoplasmic neutral lipids, whereas mildly OxLDL generated few LDs (consistent with its documented lysosomal retention) (Figure 5A). Importantly, all of these lipoproteins increased autophagic flux in macrophages (Figure 5B), and autophagy depletion in these cells resulted in diminished cholesterol efflux to apoA-I (Figure 5C).

Efflux assays to lipid-free apoA-I and HDL probe two distinct pathways of unidirectional and bidirectional cholesterol transfers, respectively (Rothblat and Phillips, 2010). Here, we assessed whether both of these efflux pathways were dependent on autophagy. Interestingly, whereas virtually all efflux to apoA-I was attributable to autophagy in AcLDL-loaded cells, approximately 30% of HDL-mediated efflux was dependent on this process (Figure 5D). It should be noted that the efflux rates measured here are similar to those in the literature,

where efflux to HDL is greater than that to apoA-I (Wang et al., 2000; Zhang et al., 2003). To assess the proportion of autophagy-mediated efflux that derives from LD cholesterol in cells incubated with apoA-I or HDL, we performed efflux experiments in the presence of an ACAT inhibitor. ACATi was included for the entire duration of these experiments, preventing cholesterol esterification and LD biogenesis (Figure S1), which results in endosomal and lysosomal cholesterol accumulation (Dove et al., 2005). Unexpectedly, the complete absence of LDs impaired efflux to apoA-I quite significantly (60% decrease), whereas efflux to HDL was slightly increased (Figures 5E and 5F), indicating that the major source of cholesterol for apoA-I-mediated efflux is the LD. Additionally, we found that lack of autophagy reduced cholesterol efflux even in the absence of LDs, suggesting a role for this pathway in enhancing efflux of lysosomal cholesterol independently of its ability to transfer LD CE to these organelles for LAL-mediated hydrolysis.

We next assessed whether our findings also apply to peritoneal macrophages. Similar to bone marrow-derived macrophages, autophagy was induced in peritoneal macrophages upon AcLDL loading, and *Atg5* deficiency reduced cholesterol efflux to apoA-I and HDL in these cells (Figure 5G). Moreover, we found that autophagy was induced in peritoneal macrophages isolated from hypercholesterolemic $apoe^{-/-}$ mice as compared to WT cells (Figure 5I). Cellular LDs were more numerous in the cytoplasm of $apoe^{-/-}$ macrophages as compared to control mice (Figure 5H), confirming the in vivo loading of these macrophages. Thus, our findings in macrophages lipid loaded in vitro appear generalizable to in vivo macrophage-loading conditions.

Lipophagy Contributes to RCT In Vivo

Because the mobilization of cholesterol from LDs is the first step in the RCT pathway, defined as the flux of cholesterol from macrophages in peripheral tissues to the liver for excretion, we reasoned that impaired efflux from autophagy-deficient macrophages would result in ineffective whole-body clearance of accumulated macrophage cholesterol. To measure RCT in vivo, we used a method developed to quantify ^{3}H-cholesterol movement from macrophages into plasma, liver, gallbladder, and feces (Wang et al., 2007; Zhang et al., 2003) over a 2 day period. Following the injection of WT or $Atg5^{-/-}$ macrophages loaded with AcLDL-derived ^{3}H-cholesterol into C57BL/6 mice, we found that the clearance of the macrophage ^{3}H-tracer was significantly reduced in mice receiving $Atg5^{-/-}$ macrophages as compared to WT macrophages (Figures 6A–6D). Thus, macrophage-specific impairment of autophagy is clearly detrimental to in vivo RCT, a process that plays a critical athero-protective role.

DISCUSSION

Here we demonstrate an important role for lysosomes in cytoplasmic CE hydrolysis in macrophage foam cells. Furthermore, we demonstrate that LDs are delivered to lysosomes via autophagy, where LAL acts to hydrolyze LD-associated CE to generate free cholesterol for efflux, a process that is specifically induced upon cholesterol loading in macrophages. Lysosomal lipolytic activity has been well studied, but it is only now realized that the source of lipids undergoing lipolysis in this compartment is not limited to extracellular lipoprotein-associated lipids reaching lysosomes via endocytosis but also extends to cytoplasmic LDs (Rodriguez-Navarro and Cuervo, 2010). CE-enriched macrophage foam cells have been shown (puzzlingly) to divert some of their cytoplasmic neutral lipids to lysosomes for hydrolysis (Avart et al., 1999). We corroborate and extend these earlier observations: sequestration of LDs by autophagosomes delivers LD CE to lysosomes, where it undergoes LAL-mediated hydrolysis to generate free cholesterol for efflux (Figure 7).

There are many models for foam cell formation in vitro, such as incubation of macrophages with AcLDL (a model modified LDL) or other atherogenic lipoproteins such as OxLDL, AgLDL, and VLDL (all of which are formed and may accumulate in pathological conditions in vivo). The AcLDL model has been extensively characterized since the late 1970s (Basu et al., 1976; Goldstein et al., 1979), and the cytoplasmic accumulation of AcLDL-derived cholesterol as CE in LDs is well documented (Brown et al., 1979; Cox et al., 2007; Itabe et al., 2000; Jerome et al., 1998; Yancey and Jerome, 1998). Multiple pieces of evidence support the premise that LDs are processed in lysosomes in the AcLDL-loaded macrophages used in our study. First, we could not detect any undigested AcLDL in lysosomes, and all of the Bodipy- or Nile Red-stained neutral lipids were surrounded by the LD coat protein, adipophilin (Figure S1). Also, adipophilin itself was localized to lysosomes (Figure 1). Furthermore, using an ACAT inhibitor during AcLDL uptake to prevent cholesterol esterification and the formation of LDs (Figure S1 confirms the lack of esterification and the lack of cytoplasmic LDs under these conditions), we found that the Lalistat 1-inhibitable efflux was abolished in the absence of LDs (Figure S2). In addition, there was diminished dissipation of adipophilin-coated neutral lipids after a 24 hr incubation of AcLDL-loaded macrophages with apoA-I in *Atg5*$^{-/-}$ macrophages relative to WT cells (Figure 4F). Moreover, efflux to apoA-I, which was nearly abolished in *Atg5*$^{-/-}$ macrophages (Figure 5E), was primarily dependent on LDs as a cholesterol source (Figure 5E, there is a 60% reduction in efflux to apoA-I in WT cells loaded with AcLDL in the presence of the ACATi as compared to WT cells loaded without ACATi in which LDs form). Finally, we show that AcLDL CE is processed very rapidly in lysosomes, and that lipoprotein-associated CE hydrolysis was equivalent in WT and *Atg5*$^{-/-}$ macrophages (Figure 4H). Thus, the decrease in cholesterol efflux from *Atg5*$^{-/-}$ cells could not result from enhanced lipoprotein CE retention in these cells as compared to WT. In any case, residual lysosomal CE after AcLDL loading is quite minimal and could not account for the decrease in efflux observed in *Atg5*$^{-/-}$ macrophages.

While cytosolic LDs are the site for CE accumulation in macrophages incubated with AcLDL, other modified lipoproteins (oxLDL, agLDL, enzymatically modified LDL) show some degree of accumulation in endolysosomal structures (Griffin et al., 2005; Schmitz and Grandl, 2009). Macrophage foam cells in human atherosclerotic lesions also display similar lipid accumulation. In early lesions, macrophage foam cells accumulate mostly cytosolic LDs (Stary et al., 1994), whereas in foam cells of advanced atherosclerotic plaques much of the cholesterol is trapped in lysosomes (Jerome, 2006). The evidence that autophagy is induced with lipid loading and actively mobilizes LD CE indicates that autophagy and LAL may be particularly relevant to the reversal of early lesions. Our results also support a possible role in the regression of advanced lesions. As seen from Figure 5E, even in the absence of any cytoplasmic LDs, there is an autophagy-attributable efflux to apoA-I.

Here, we clearly establish that autophagy-mediated efflux is closely linked to the ATP-binding cassette (ABC) transporter ABCA1, which itself is linked to the endosomal/lysosomal cholesterol pools. In the absence of LDs and autophagy, efflux to apoA-I is nearly completely abolished, whereas this is not the case for efflux to HDL (Figures 5E and 5F). This implies that autophagy-mediated efflux is primarily ABCA1 dependent, since efflux to lipid-poor apoA-I is completely dependent on ABCA1, whereas this transporter contributes to a small proportion of HDL-mediated efflux (Wang et al., 2000). Whereas ABCA1 mediates a unidirectional transport, mostly to apoA-I (Wang et al., 2000), HDL-mediated efflux is a bidirectional, diffusional process that involves multiple transporters (Rothblat and Phillips, 2010) and represents a complex pathway for which the contribution of autophagy remains to be studied in greater detail. Macrophage ABCA1 is responsible for approximately 50% of total RCT in vivo (Wang et al., 2007), but its contribution to efflux to HDL is low in vitro (Wang et al., 2000). In agreement with these findings, we observed a

modest decrease in efflux to HDL in *Atg5*$^{-/-}$ macrophages in vitro (Figures 5D and 5F) and a more pronounced effect of macrophage-specific autophagy deletion on excretion of macrophage ^{3}H-cholesterol in vivo (Figure 6).

Autophagy is markedly elevated in macrophages in response to lipid loading (Figure 3). Fittingly, under lipid-loaded conditions, apoA-I/ABCA1 retroendocytosis (a process by which apoA-I acquires lipid from late endosomal/lysosomal compartments) contributes to efficient cholesterol efflux, whereas in the absence of cholesterol loading, lipidation of apoA-I occurs primarily at the plasma membrane (Azuma et al., 2009). Additionally, ABCA1 expression is increased in response to cholesterol loading, both transcriptionally via the liver X receptor (LXR) (Beaven and Tontonoz, 2006) and posttranscriptionally by miR-33 (Rayner et al., 2010). Using an LXR activator (T0901317) to maximally stimulate ABCA1 activity dramatically enhances cholesterol efflux to apoA-I; in Lalistat 1-treated and *Atg5*$^{-/-}$ macrophages, however, T0901317 fails to increase efflux to apoA-I, given that cholesterol delivery to ABCA1 under these conditions is seemingly limiting (Figure S3).

Our observation that the expansion of intracellular cholesterol pools triggers autophagy seems contradictory to previous reports linking the depletion of cellular cholesterol levels to autophagy induction in fibroblasts (Cheng et al., 2006) and in hepatocytes (Seo et al., 2011). However, increased LD delivery to lysosomes has been shown to occur in response to starvation as well as triglyceride loading in hepatocytes (Singh et al., 2009a). Importantly, the prolonged presence of lipogenic stimuli ultimately results in inhibition of autophagosome clearance by lysosomes. Whereas a moderate cholesterol increase was shown to increase autophagic flow, the fusogenic ability of the autophagic/lysosomal compartments is attenuated in conditions of chronic lipid exposure (Koga et al., 2010). It will be interesting to determine whether autophagy becomes defective in macrophages derived from advanced atherosclerotic lesions as compared to early foam cells. Impairment of autophagy-mediated cholesterol clearance in advanced foam cells would be predicted to exacerbate lipid accumulation in these lesions, given that RCT from *Atg5*$^{-/-}$ macrophages is significantly reduced in vivo (Figure 6).

In summary, we demonstrate an important role for autophagy in cholesterol efflux from macrophage foam cells (Figure 7). We demonstrate that this pathway is important for macrophage LD clearance in primary bone marrow-derived and peritoneal macrophages. Autophagy-dependent macrophage cholesterol efflux is an ABCA1-mediated process that is enhanced by the uptake of various atherogenic lipoproteins such as AcLDL, OxLDL, AgLDL, and VLDL in vitro. In addition, we report that the autophagy pathway is induced in peritoneal macrophages loaded in vivo. Based on the finding that macrophage-specific autophagy deficiency is detrimental to RCT, impairment of macrophage autophagy would be expected to promote atherosclerotic lipid accumulation. Activators of autophagy, which trigger autophagy via mTOR inhibition, are emerging as promising agents to treat coronary heart disease (Jia and Hui, 2009). The systemic administration of mTOR inhibitors has been shown to prevent development of atherosclerosis, attenuate plaque progression, and reduce cholesterol content in the aortic arch in atherogenic mouse models (Basso et al., 2003; Mueller et al., 2008; Pakala et al., 2005). Although further studies are required to establish a correlation between the regulation of autophagy in macrophages and atherosclerosis, our results suggest that the controlled stimulation of autophagy may provide therapeutic potential to enhance macrophage cholesterol efflux and promote RCT.

EXPERIMENTAL PROCEDURES

Cell Culture

Bone marrow cells were flushed from the femurs of C57BL/6 mice or from *Atg5*$^{-/-}$/*LDLR*$^{-/-}$ and *LDLR*$^{-/-}$ mice on a C57BL/6 background and differentiated into macrophages by incubation in L929-conditioned media for 7 days. Peritoneal macrophages from *Atg5*$^{-/-}$/*LDLR*$^{-/-}$ and *LDLR*$^{-/-}$ were harvested 4 days after i.p. injection of methyl-BSA in mice previously immunized with this antigen. For in vivo macrophage cholesterol loading, *apoe*$^{-/-}$ or WT mice on a C57BL/6 background were placed on a Western diet for 2 weeks, and peritoneal macrophages were harvested 3 days after thioglycolate injection.

Lipoprotein Preparation

HDL, VLDL, and LDL were isolated by sequential density ultracentrifugation. LDL was acetylated by repetitive additions of acetic anhydride, aggregated by vortexing, or oxidized by incubation with $CuSO_4$ for 24 hr.

Cholesterol Efflux

Macrophages were incubated for 30 hr in media containing 50 μg/mL of lipoproteins that were preincubated with ^{3}H-cholesterol (5 μCi/mL). Cells were washed and equilibrated overnight in 2 mg/mL BSA media, and cholesterol efflux was determined in the presence or absence of human recombinant apoA-I (50 μg/mL) or HDL (50 μg/mL) in serum-free media with the indicated reagent (paraoxon 100 μM, chloroquine 30 μM, vinblastine 30 μM, bafilomycin 10 nM, ACATi 10 μg/mL, Lalistat 1 10 μM) for 18–24 hr (unless otherwise specified). Efflux is expressed as a percentage of ^{3}H-cholesterol in medium/(^{3}H-cholesterol in medium+^{3}H-cholesterol in cells) × 100%. Efflux to apoA-I or HDL was calculated by subtracting effluxes of the wells without apoA-I or HDL from those containing apoA-I or HDL.

In Vivo RCT Studies

Macrophage RCT experiments were carried out similarly to that previously described (Wang et al., 2007). Macrophages from WT or *Atg5*$^{-/-}$ mice were loaded with ^{3}H-cholesterol-AcLDL as described above for cholesterol effluxes, and 200 μL of cell preparations (~5 × 10^6 cells containing ~2 × 10^6CPM) were injected subfascially in the lumbar region of C57BL/6 mice. Blood was collected at 24 hr via the saphenous vein and at 48 hr via cardiac puncture of anesthetized mice. Plasma was used for liquid scintillation counting. At 48 hr, gallbladders were emptied, and livers were removed for scintillation counting. Feces were collected over a 48 hr period, and total feces radioactivity (of equivalent wet weight) was measured. All ^{3}H-tracer measurements are expressed relative to the injected amount.

Lipid Measurements

The Biovision Cholesterol Quantitation Kit was used to determine cellular mass of cholesterol and CEs. Variations in CE are expressed as percent hydrolysis or as fold change relative to control, calculated as follows: % hydrolysis = $(CE_i - CE_f)/(CE_i)*100$, where CE_i represents the CE mass immediately after AcLDL loading, and CE_f represents the CE mass after the cells were incubated for 24 hr with apoA-I; fold change = (% hydrolysis sample/% hydrolysis control).

CE Quantification by TLC

Total lipids were extracted and separated by thin-layer chromatography (TLC) using a nonpolar solvent system for separation of cholesterol and CE. The bands corresponding to cholesterol and CE were excised and counted for radioactivity.

^{3}H-Cholesterol and ^{14}C-Oleic Acid Esterification

Macrophages were incubated with ^{3}H-cholesterol-AcLDL and 0.1mMsodium ^{14}C-oleate-albumin complex for 30 hr, in the presence or absence of ACATi. The ^{3}H and ^{14}C labels were quantified in the CE fraction after TLC.

Western Blotting

Cells were lysed in Laemmli sample buffer (Bio-Rad). Total protein samples were electrophoresed on precast 4%–20% or 18% SDS-polyacrylamide gels (Invitrogen) and transferred to nitrocellulose or PVDF membranes at 125V for 2 hr. Membranes were probed with the indicated antibodies, which were detected using HRP-based chemiluminescence.

Lipid Droplet Isolation

LDs were isolated from AcLDL-loaded macrophages by density gradient centrifugation, and whole LD fractions were used for SDS-PAGE.

Fluorescence Microscopy

Neutral lipids were stained using Bodipy 493/503 or Nile Red. For live cell imaging, AcLDL-loaded macrophages were incubated with Bodipy (10 μg/mL) with or without LysoTracker Red (50 nM) for 30 min prior to visualization, or with 10 μg/mL of the BSA conjugate 4 hr prior to labeling with Bodipy. For immunofluorescence, cells were fixed in 4% PFA, blocked/permeabilized in 2.5% BSA/0.1% Triton X-100, and stained with the indicated primary antibodies for 1 hr at 37°C. Fluorophore-conjugated secondary antibodies were incubated in the presence of Nile Red (50 ng/mL) to stain neutral lipids. Confocal images and movies were obtained using an Olympus IX80 FV1000 confocal microscope with appropriate lasers.

Electron Microscopy

AcLDL-loaded macrophages were fixed in 1.6% glutaraldehyde prior to post-fixation in osmium tetroxide and uranyl acetate en bloc staining. Samples were processed and embedded in Spurr epoxy resin, thin sectioned, and counterstained with lead citrate. Digital images were obtained with a JEOL 1230 TEM at 60 kV adapted with a 2000 × 2000 pixel bottom-mount CCD digital camera and AMT software.

LC3 Immunogold Labeling

A pre-embedding method followed by silver enhancement was used for immunoelectron microscopy. AcLDL-loaded macrophages were fixed in 4% paraformaldehyde and 0.1% glutaraldehyde in PBS. Cells were permeabilized, blocked, and immunolabeled with anti-LC3 and incubated with anti-rabbit IgG conjugated to colloidal gold (1.4 nm diameter). Cells were postfixed with 1% glutaraldehyde, and the gold was intensified using the HQ Silver Enhancement Kit (Nanoprobes). Cells were dehydrated with a graded series of ethanol, embedded, counterstained, and imaged.

Statistical Analysis

All presented values are mean ± SEM. Statistical significance of the differences between groups was determined using the GraphPad InStat software.

Supplementary Material

Refer to Web version on PubMed Central for supplementary material.

Acknowledgments

We thank Paul Helquist, Casey Cosner (Notre Dame University), Fred Maxfield, and Anton Rosenbaum (Weill Cornell Medical College) for providing us with the LAL inhibitor Lalistat 1. We also thank Peter Rippstein and Junhui Tan for their assistance with the electron microscopy, as well as members of the Tabas lab (especially Christopher Scull) for their resourcefulness over the course of the *Atg5*−/− experiments. We thank Ruth McPherson for critical reading of the manuscript. Finally, we would like to acknowledge the constructive criticisms and comments of reviewers that led to key insights in the mechanisms of macrophage autophagy-mediated cholesterol efflux. This work was supported by grants from CIHR and the Heart and Stroke Foundation of Ontario (to Y.L.M.) and by NIH grant HL057560 (to I.T.). M.O. is the recipient of a Vanier Canada Graduate Scholarship from CIHR.

REFERENCES

Avart SJ, Bernard DW, Jerome WG, Glick JM. Cholesteryl ester hydrolysis in J774 macrophages occurs in the cytoplasm and lysosomes. J. Lipid Res. 1999; 40:405–414. [PubMed: 10064728]

Azuma Y, Takada M, Shin HW, Kioka N, Nakayama K, Ueda K. Retroendocytosis pathway of ABCA1/apoA-I contributes to HDL formation. Genes Cells. 2009; 14:191–204. [PubMed: 19170766]

Baerga R, Zhang Y, Chen PH, Goldman S, Jin S. Targeted deletion of autophagy-related 5 (atg5) impairs adipogenesis in a cellular model and in mice. Autophagy. 2009; 5:1118–1130. [PubMed: 19844159]

Basso MD, Nambi P, Adelman SJ. Effect of sirolimus on the cholesterol content of aortic arch in ApoE knockout mice. Transplant. Proc. 2003; 35:3136–3138. [PubMed: 14697997]

Basu SK, Goldstein JL, Anderson GW, Brown MS. Degradation of cationized low density lipoprotein and regulation of cholesterol metabolism in homozygous familial hypercholesterolemia fibroblasts. Proc. Natl. Acad. Sci. USA. 1976; 73:3178–3182. [PubMed: 184464]

Beaven SW, Tontonoz P. Nuclear receptors in lipid metabolism: targeting the heart of dyslipidemia. Annu. Rev. Med. 2006; 57:313–329. [PubMed: 16409152]

Brown MS, Goldstein JL, Krieger M, Ho YK, Anderson RG. Reversible accumulation of cholesteryl esters in macrophages incubated with acetylated lipoproteins. J. Cell Biol. 1979; 82:597–613. [PubMed: 229107]

Brown MS, Ho YK, Goldstein JL. The cholesteryl ester cycle in macrophage foam cells. Continual hydrolysis and re-esterification of cytoplasmic cholesteryl esters. J. Biol. Chem. 1980; 255:9344–9352. [PubMed: 7410428]

Cheng J, Ohsaki Y, Tauchi-Sato K, Fujita A, Fujimoto T. Cholesterol depletion induces autophagy. Biochem. Biophys. Res. Commun. 2006; 351:246–252. [PubMed: 17056010]

Cox BE, Griffin EE, Ullery JC, Jerome WG. Effects of cellular cholesterol loading on macrophage foam cell lysosome acidification. J. Lipid Res. 2007; 48:1012–1021. [PubMed: 17308299]

Cuervo AM, Dice JF, Knecht E. A population of rat liver lysosomes responsible for the selective uptake and degradation of cytosolic proteins. J. Biol. Chem. 1997; 272:5606–5615. [PubMed: 9038169]

Dove DE, Su YR, Zhang W, Jerome WG, Swift LL, Linton MF, Fazio S. ACAT1 deficiency disrupts cholesterol efflux and alters cellular morphology in macrophages. Arterioscler. Thromb. Vasc. Biol. 2005; 25:128–134. [PubMed: 15499044]

Farese RV Jr, Walther TC. Lipid droplets finally get a little R-E-S-P-E-C-T. Cell. 2009; 139:855–860. [PubMed: 19945371]

Ghosh S, Zhao B, Bie J, Song J. Macrophage cholesteryl ester mobilization and atherosclerosis. Vascul. Pharmacol. 2010; 52:1–10. [PubMed: 19878739]

Goldstein JL, Faust DS Jr, Beaudet AL, Brown MS. Role of lysosomal acid lipase in the metabolism of plasma low density lipoprotein. Observations in cultured fibroblasts from a patient with cholesteryl ester storage disease. J. Biol. Chem. 1975; 250:8487–8495. [PubMed: 172501]

Goldstein JL, Ho YK, Basu SK, Brown MS. Binding site on macrophages that mediates uptake and degradation of acetylated low density lipoprotein, producing massive cholesterol deposition. Proc. Natl. Acad. Sci. USA. 1979; 76:333–337. [PubMed: 218198]

Griffin EE, Ullery JC, Cox BE, Jerome WG. Aggregated LDL and lipid dispersions induce lysosomal cholesteryl ester accumulation in macrophage foam cells. J. Lipid Res. 2005; 46:2052–2060. [PubMed: 16024919]

Ileperuma NR, Marshall SD, Squire CJ, Baker HM, Oakeshott JG, Russell RJ, Plummer KM, Newcomb RD, Baker EN. High-resolution crystal structure of plant carboxylesterase AeCXE1, from Actinidia eriantha, and its complex with a high-affinity inhibitor paraoxon. Biochemistry. 2007; 46:1851–1859. [PubMed: 17256879]

Itabe H, Suzuki K, Tsukamoto Y, Komatsu R, Ueda M, Mori M, Higashi Y, Takano T. Lysosomal accumulation of oxidized phosphatidylcholine-apolipoprotein B complex in macrophages: intracellular fate of oxidized low density lipoprotein. Biochim. Biophys. Acta. 2000; 1487:233–245. [PubMed: 11018475]

Jerome WG. Advanced atherosclerotic foam cell formation has features of an acquired lysosomal storage disorder. Rejuvenation Res. 2006; 9:245–255. [PubMed: 16706652]

Jerome WG, Cash C, Webber R, Horton R, Yancey PG. Lysosomal lipid accumulation from oxidized low density lipoprotein is correlated with hypertrophy of the Golgi apparatus and trans-Golgi network. J. Lipid Res. 1998; 39:1362–1371. [PubMed: 9684738]

Jia L, Hui RT. Everolimus, a promising medical therapy for coronary heart disease? Med. Hypotheses. 2009; 73:153–155. [PubMed: 19375241]

Kabeya Y, Mizushima N, Ueno T, Yamamoto A, Kirisako T, Noda T, Kominami E, Ohsumi Y, Yoshimori T. LC3, a mammalian homologue of yeast Apg8p, is localized in autophagosome membranes after processing. EMBO. J. 2000; 19:5720–5728. [PubMed: 11060023]

Khera AV, Rader DJ. Future therapeutic directions in reverse cholesterol transport. Curr. Atheroscler. Rep. 2010; 12:73–81. [PubMed: 20425274]

Klionsky DJ. The molecular machinery of autophagy: unanswered questions. J. Cell Sci. 2005; 118:7–18. [PubMed: 15615779]

Koga H, Kaushik S, Cuervo AM. Altered lipid content inhibits autophagic vesicular fusion. FASEB. J. 2010; 24:3052–3065. [PubMed: 20375270]

Kovsan J, Bashan N, Greenberg A, Rudich A. Potential role of autophagy in modulation of lipid metabolism. Am J Physiol. Endocrinol. Metab. 2009; 289:E1–E7. [PubMed: 19887596]

Lepine S, Allegood JC, Park M, Dent P, Milstien S, Spiegel S. Sphingosine-1-phosphate phosphohydrolase-1 regulates ER stress-induced autophagy. Cell Death Differ. 2010; 18:350–361. [PubMed: 20798685]

Listenberger LL, Brown DA. Fluorescent detection of lipid droplets and associated proteins. Curr. Protoc. Cell Biol. 2007 Chapter 24, Unit 24.2.

Mizushima N, Yamamoto A, Hatano M, Kobayashi Y, Kabeya Y, Suzuki K, Tokuhisa T, Ohsumi Y, Yoshimori T. Dissection of autophagosome formation using Apg5-deficient mouse embryonic stem cells. J. Cell Biol. 2001; 152:657–668. [PubMed: 11266458]

Mueller MA, Beutner F, Teupser D, Ceglarek U, Thiery J. Prevention of atherosclerosis by the mTOR inhibitor everolimus in LDLR−/− mice despite severe hypercholesterolemia. Atherosclerosis. 2008; 198:39–48. [PubMed: 17980369]

Murphy S, Martin S, Parton RG. Lipid droplet-organelle interactions; sharing the fats. Biochim. Biophys. Acta. 2008; 1791:441–447. [PubMed: 18708159]

Pakala R, Stabile E, Jang GJ, Clavijo L, Waksman R. Rapamycin attenuates atherosclerotic plaque progression in apolipoprotein E knockout mice: inhibitory effect on monocyte chemotaxis. J. Cardiovasc. Pharmacol. 2005; 46:481–486. [PubMed: 16160601]

Paul A, Chang BH, Li L, Yechoor VK, Chan L. Deficiency of adipose differentiation-related protein impairs foam cell formation and protects against atherosclerosis. Circ. Res. 2008; 102:1492–1501. [PubMed: 18483409]

Rayner KJ, Suarez Y, Davalos A, Parathath S, Fitzgerald ML, Tamehiro N, Fisher EA, Moore KJ, Fernandez-Hernando C. MiR-33 contributes to the regulation of cholesterol homeostasis. Science. 2010; 328:1570–1573. [PubMed: 20466885]

Rodriguez-Navarro JA, Cuervo AM. Autophagy and lipids: tightening the knot. Semin. Immunopath. 2010; 32:343–353.

Rosenbaum AI, Rujoi M, Huang AY, Du H, Grabowski GA, Maxfield FR. Chemical screen to reduce sterol accumulation in Niemann-Pick C disease cells identifies novel lysosomal acid lipase inhibitors. Biochim. Biophys. Acta. 2009; 1791:1155–1165. [PubMed: 19699313]

Rosenbaum AI, Cosner CC, Mariani CJ, Maxfield FR, Wiest O, Helquist P. Thiadiazole carbamates: potent inhibitors of lysosomal acid lipase and potential Niemann-pick type C disease therapeutics. J. Med. Chem. 2010; 53:5281–5289. [PubMed: 20557099]

Rothblat GH, Phillips MC. High-density lipoprotein heterogeneity and function in reverse cholesterol transport. Curr. Opin. Lipidol. 2010; 21:229–238. [PubMed: 20480549]

Sankaranarayanan S, de la Llera-Moya M, Drazul-Schrader D, Asztalos BF, Weibel GL, Rothblat GH. Importance of macrophage cholesterol content on the flux of cholesterol mass. J. Lipid Res. 2010; 51:3243–3249. [PubMed: 20713652]

Schmitz G, Grandl M. Endolysosomal phospholipidosis and cytosolic lipid droplet storage and release in macrophages. Biochim. Biophys. Acta. 2009; 1791:524–539. [PubMed: 19146988]

Seo YK, Jeon TI, Chong HK, Biesinger J, Xie X, Osborne TF. Genome-wide localization of SREBP-2 in hepatic chromatin predicts a role in autophagy. Cell Metab. 2011; 13:367–375. [PubMed: 21459322]

Shashkin P, Dragulev B, Ley K. Macrophage differentiation to foam cells. Curr. Pharm. Des. 2005; 11:3061–3072. [PubMed: 16178764]

Shibata M, Yoshimura K, Furuya N, Koike M, Ueno T, Komatsu M, Arai H, Tanaka K, Kominami E, Uchiyama Y. The MAP1-LC3 conjugation system is involved in lipid droplet formation. Biochem. Biophys. Res. Commun. 2009; 382:419–423. [PubMed: 19285958]

Singh R, Kaushik S, Wang Y, Xiang Y, Novak I, Komatsu M, Tanaka K, Cuervo AM, Czaja MJ. Autophagy regulates lipid metabolism. Nature. 2009a; 458:1131–1135. [PubMed: 19339967]

Singh R, Xiang Y, Wang Y, Baikati K, Cuervo AM, Luu YK, Tang Y, Pessin JE, Schwartz GJ, Czaja MJ. Autophagy regulates adipose mass and differentiation in mice. J. Clin. Invest. 2009b; 119:3329–3339. [PubMed: 19855132]

Stary HC, Chandler AB, Glagov S, Guyton JR, Insull W Jr, Rosenfeld ME, Schaffer SA, Schwartz CJ, Wagner WD, Wissler RW. A definition of initial, fatty streak, and intermediate lesions of atherosclerosis. A report from the Committee on Vascular Lesions of the Council on Arteriosclerosis, American Heart Association. Arterioscler. Thromb. 1994; 14:840–856. [PubMed: 8172861]

Tanida I. Autophagosome formation and molecular mechanism of autophagy. Antioxid. Redox. Signal. 2010 Published online December 4 2010.

Tanida I, Minematsu-Ikeguchi N, Ueno T, Kominami E. Lysosomal turnover, but not a cellular level, of endogenous LC3 is a marker for autophagy. Autophagy. 2005; 1:84–91. [PubMed: 16874052]

Tooze SA, Yoshimori T. The origin of the autophagosomal membrane. Nat. Cell Biol. 2010; 12:831–835. [PubMed: 20811355]

Wang N, Silver DL, Costet P, Tall AR. Specific binding of ApoA-I, enhanced cholesterol efflux, and altered plasma membrane morphology in cells expressing ABC1. J. Biol. Chem. 2000; 275:33053–33058. [PubMed: 10918065]

Wang MD, Franklin V, Marcel YL. In vivo reverse cholesterol transport from macrophages lacking ABCA1 expression is impaired. Arterioscler. Thromb. Vasc. Biol. 2007; 27:1837–1842. [PubMed: 17541020]

Wei E, Gao W, Lehner R. Attenuation of adipocyte triacylglycerol hydrolase activity decreases basal fatty acid efflux. J. Biol. Chem. 2007; 282:8027–8035. [PubMed: 17237500]

Weidberg H, Shvets E, Elazar Z. Lipophagy: selective catabolism designed for lipids. Dev. Cell. 2009; 16:628–630. [PubMed: 19460339]

Yancey PG, Jerome WG. Lysosomal sequestration of free and esterified cholesterol from oxidized low density lipoprotein in macrophages of different species. J. Lipid Res. 1998; 39:1349–1361. [PubMed: 9684737]

Zhang Y, Goldman S, Baerga R, Zhao Y, Komatsu M, Jin S. Adipose-specific deletion of autophagy-related gene 7 (atg7) in mice reveals a role in adipogenesis. Proc. Natl. Acad. Sci. USA. 2009; 106:19860–19865. [PubMed: 19910529]

Zhang Y, Zanotti I, Reilly MP, Glick JM, Rothblat GH, Rader DJ. Overexpression of apolipoprotein A-I promotes reverse transport of cholesterol from macrophages to feces in vivo. Circulation. 2003; 108:661–663. [PubMed: 12900335]

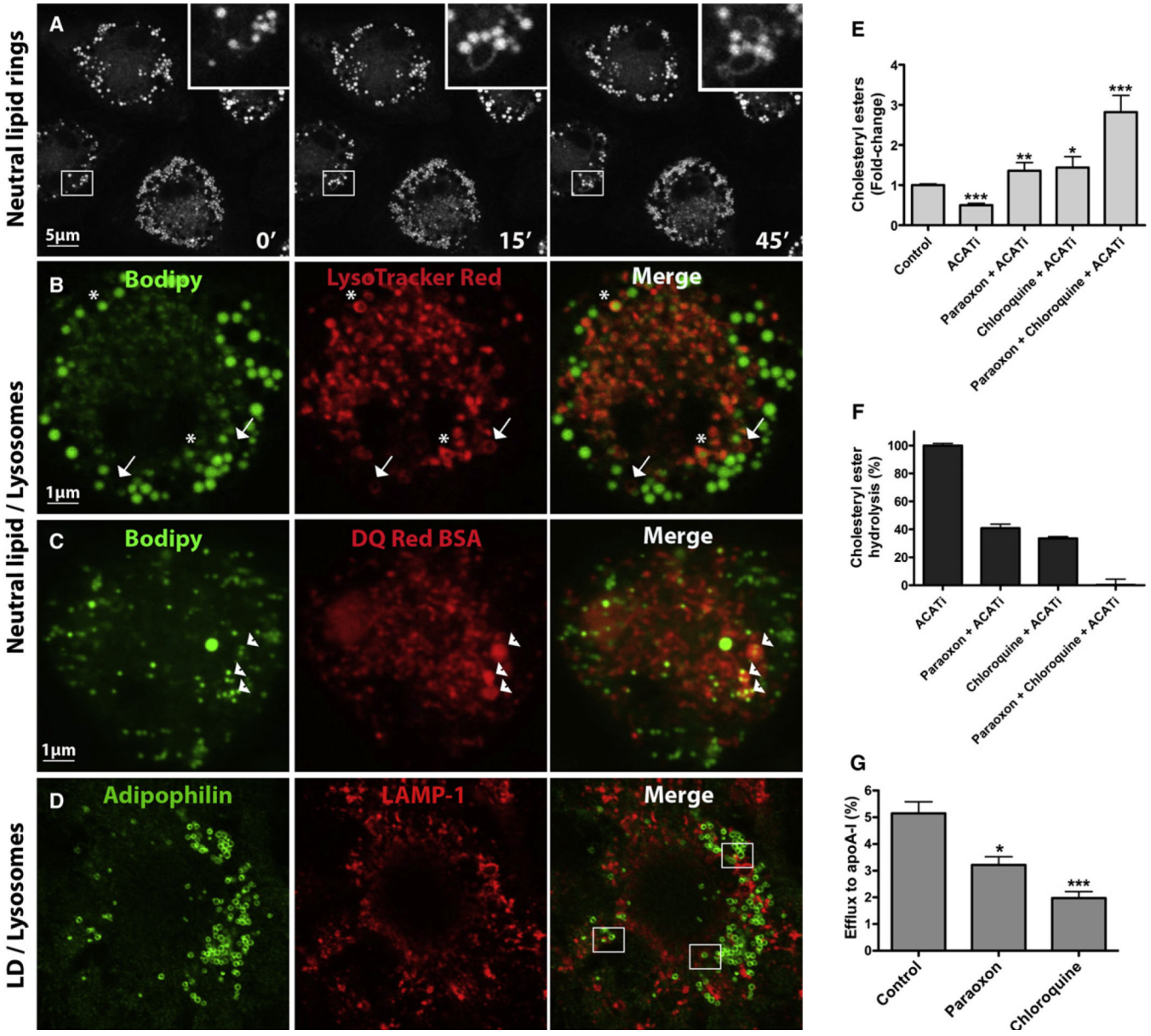

Figure 1. LDs Surround Neutral Lipid Rings and Colocalize with Lysosomes; Inhibition of Lysosomal Function Reduces CE Hydrolysis and Cholesterol Efflux

(A and B) BMDMs were loaded with AcLDL-derived cholesterol for 30 hr, equilibrated overnight in BSA media, and then incubated with media containing Bodipy (10 μg/mL) with or without LysoTracker Red (50 nM) for 30 min prior to visualization.

(C) Cells were cholesterol loaded as above and then incubated with a BSA conjugate prior to labeling with Bodipy.

(D) Colocalization between the macrophage LD coat protein adipophilin and LAMP-1-positive lysosomes in AcLDL-loaded macrophages.

(E and F) Cellular CE (E) and CE hydrolysis (F) were measured in AcLDL-loaded cells treated with paraoxon or chloroquine for 24 hr in the presence of apoA-I, with or without ACATi. Variations in CE are expressed as fold change relative to control (E) or as a percent CE hydrolysed in 24 hr (F). ***$p < 0.0001$, **$p < 0.001$, or *$p < 0.005$ compared to ACATi, and ACATi was compared to control.

(G) BMDMs were loaded with ^{3}H-cholesterol-AcLDL for 30 hr and equilibrated overnight, and efflux to apoA-I was measured for 24 hr in the presence or absence of paraoxon or chloroquine.

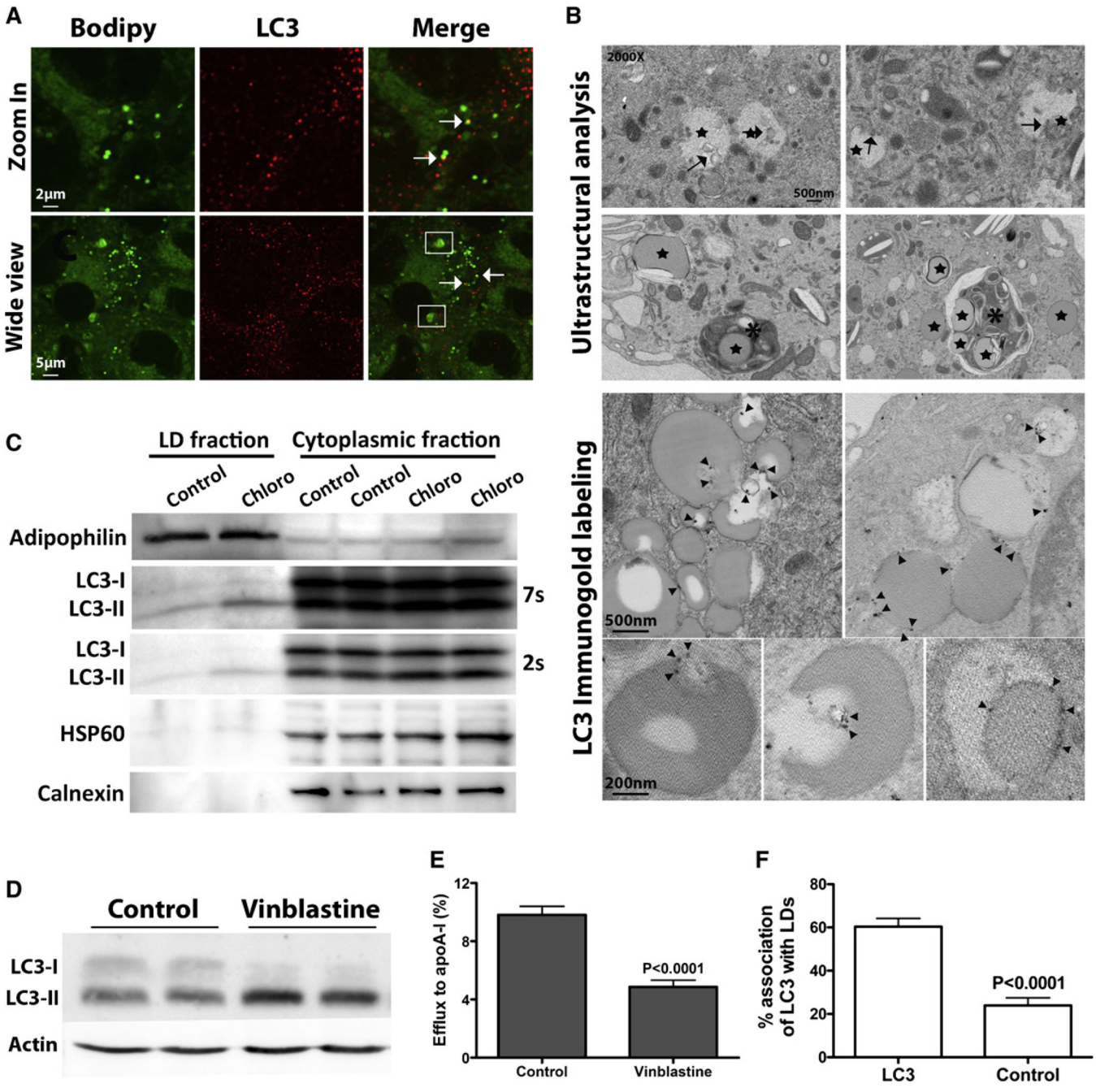

Figure 2. Autophagy Is Implicated in Cytoplasmic LD Degradation

(A–C) In lipid-loaded BMDMs, direct association of autophagomes with LDs is observed by immunofluorescence (A), electron microscopy (B), and in an isolated LD fraction (C).

(D) Vinblastine treatment inhibits autophagosome degradation, as shown by elevated LC3-II.

(E) Inhibition of autophagy by vinblastine treatment during cholesterol efflux decreases efflux to apoA-I.

(F) Quantification of LDs containing gold particles (cells immunostained with LC3 are compared to the secondary antibody alone negative control).

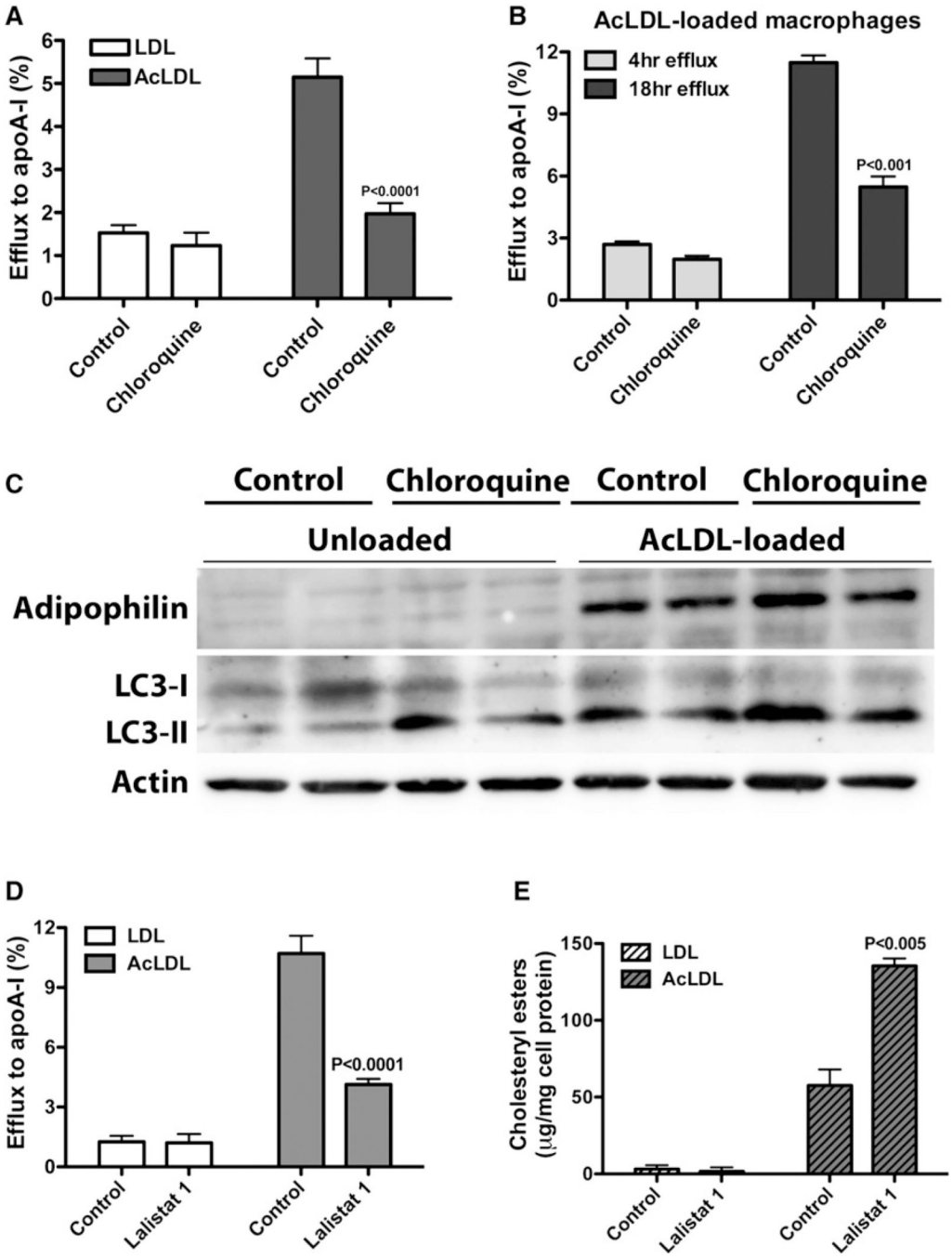

Figure 3. Autophagy Is Induced in Response to Lipid Loading, and LAL Mediates LD Catabolism

(A) Chloroquine inhibits cholesterol efflux in macrophage foam cells, but not in unloaded cells.

(B) Chloroquine has no effect on cholesterol efflux at an early time point, but impairs cholesterol efflux upon prolonged inhibition of lysosomal function.

(C) Autophagic flux is induced in lipid-loaded macrophages.

(D and E) Effect of LAL inhibition on cholesterol efflux (D) and cellular CE mass (E) in unloaded versus lipid-loaded macrophages.

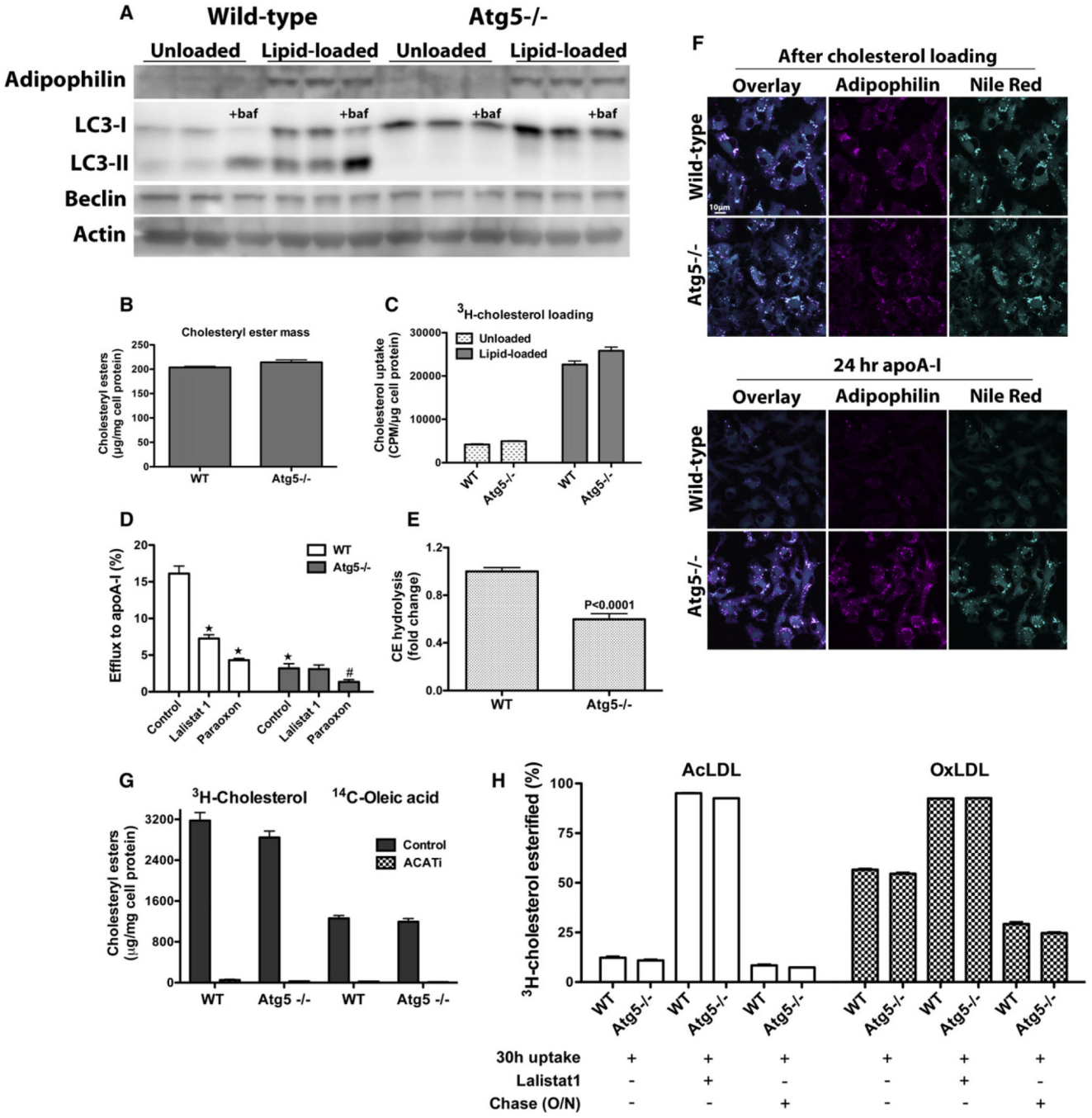

Figure 4. Ablation of Autophagy Impairs LD Delivery to Lysosomes for LAL-Mediated CE Hydrolysis in Macrophage Foam Cells

(A) *Atg5* deletion in macrophages impairs LC3-I maturation to LC3-II, and autophagy cannot ensue.

(B and C) Cholesterol loading is similar in WT and $Atg5^{-/-}$ macrophages, as recorded by mass measurements (B) and ^{3}H-cholesterol uptake (C).

(D) Cholesterol efflux to apoA-I is impaired in $Atg5^{-/-}$ lipid-loaded macrophages; LAL inhibition reduces cholesterol efflux in WT, but not $Atg5^{-/-}$, macrophages. ★$p < 0.0001$ relative to WT control, and #$p < 0.05$ relative to $Atg5^{-/-}$ control.

(E) CE hydrolysis in lipid-loaded WT and *Atg5*$^{-/-}$ macrophages over 24 hr in the presence of apoA-I, expressed as a fold change relative to the WT control (cellular CE mass was measured before and after cholesterol efflux, and resulting percent hydrolysis was normalized to that of WT).
(F) Autophagy-deficient macrophages exhibit impaired LD catabolism. Lipid-loaded WT or *Atg5*$^{-/-}$ macrophages were immediately fixed for fluorescence microscopy after AcLDL loading or after a 24 hr incubation with media containing lipid-poor apoA-I in the presence of an ACAT inhibitor. Neutral lipids were stained with Nile Red.
(G) AcLDL-derived ^{3}H-cholesterol is esterified to ^{14}C-oleic acid to the same extent in WT and $^{Atg5-/-}$ macrophages. In the absence of the ACATi, esterification of the ^{3}H and ^{14}C labels parallels each other and is equivalent in WT and *Atg5*$^{-/-}$ cells. When the ER-resident ACAT is inhibited by ACATi, esterification of both the ^{3}H and ^{14}C labels is abolished.
(H) Degradation of lipoprotein ^{3}H-cholesteryl oleate occurs at the same rate in WT and *Atg5*$^{-/-}$ macrophages. Macrophages were loaded with AcLDL or OxLDL containing ^{3}H-cholesteryl oleate in the presence or absence of Lalistat 1 to inhibit LAL, followed by an O/N equilibration or not. All experiments were performed in the presence of the ACATi to prevent re-esterification of the liberated ^{3}H-cholesterol.

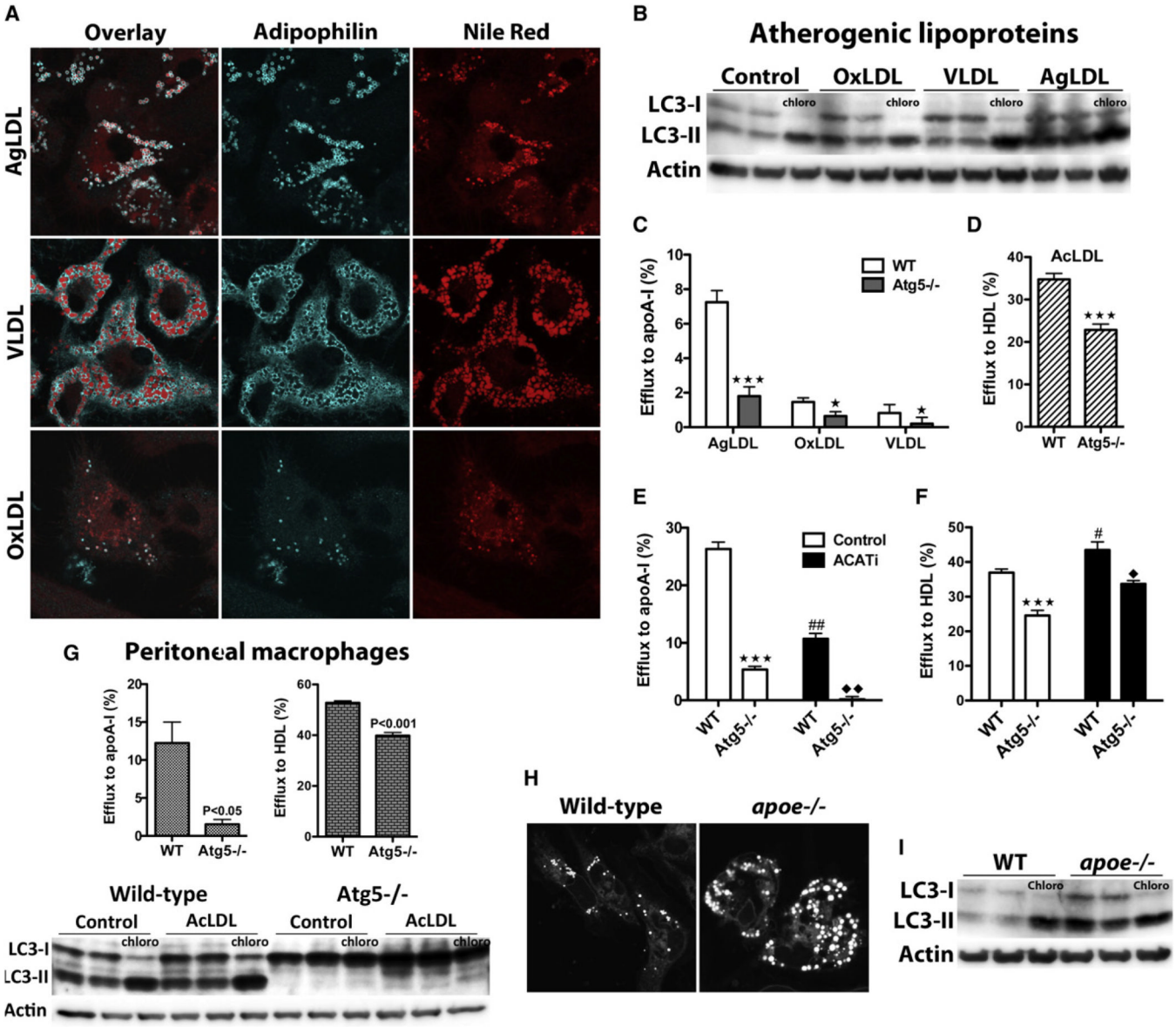

Figure 5. Enhanced Autophagy in Response to Various Atherogenic Lipoproteins and in Peritoneal Macrophages from Hypercholesterolemic Mice

(A) LD genesis in bone marrow-derived macrophages exposed to AgLDL, VLDL, and OxLDL.

(B) Elevated autophagic flux in response to atherogenic lipoproteins.

(C) Impaired efflux to apoA-I in *atg5*$^{-/-}$ macrophages loaded with AgLDL, VLDL, and OxLDL.

(D) Atg5 ablation reduces cholesterol efflux to HDL in AcLDL-loaded macrophages.

(E and F) Efflux to apoA-I (E) and HDL (F) in WT and *Atg5*$^{-/-}$ macrophages with (control) or without (ACATi) cytoplasmic LDs.

(C–F) ★★★p < 0.0001 or ★p < 0.05 relative to WT control, and ##p < 0.001 or #p < 0.05 for ACATi-treated WT cells relative to WT control, and ♦♦p < 0.001 or ♦p < 0.05 for ACATi-treated *Atg5*$^{-/-}$ cells relative to ACATi-treated WT cells.

(G) Autophagy mediates cholesterol efflux in peritoneal macrophages.

(H) Peritoneal macrophages isolated from hypercholesterolemic *apoe*$^{-/-}$ mice contain more LDs than their WT counterparts.
(I) Autophagy levels are elevated in peritoneal macrophages lipid loaded in vivo.

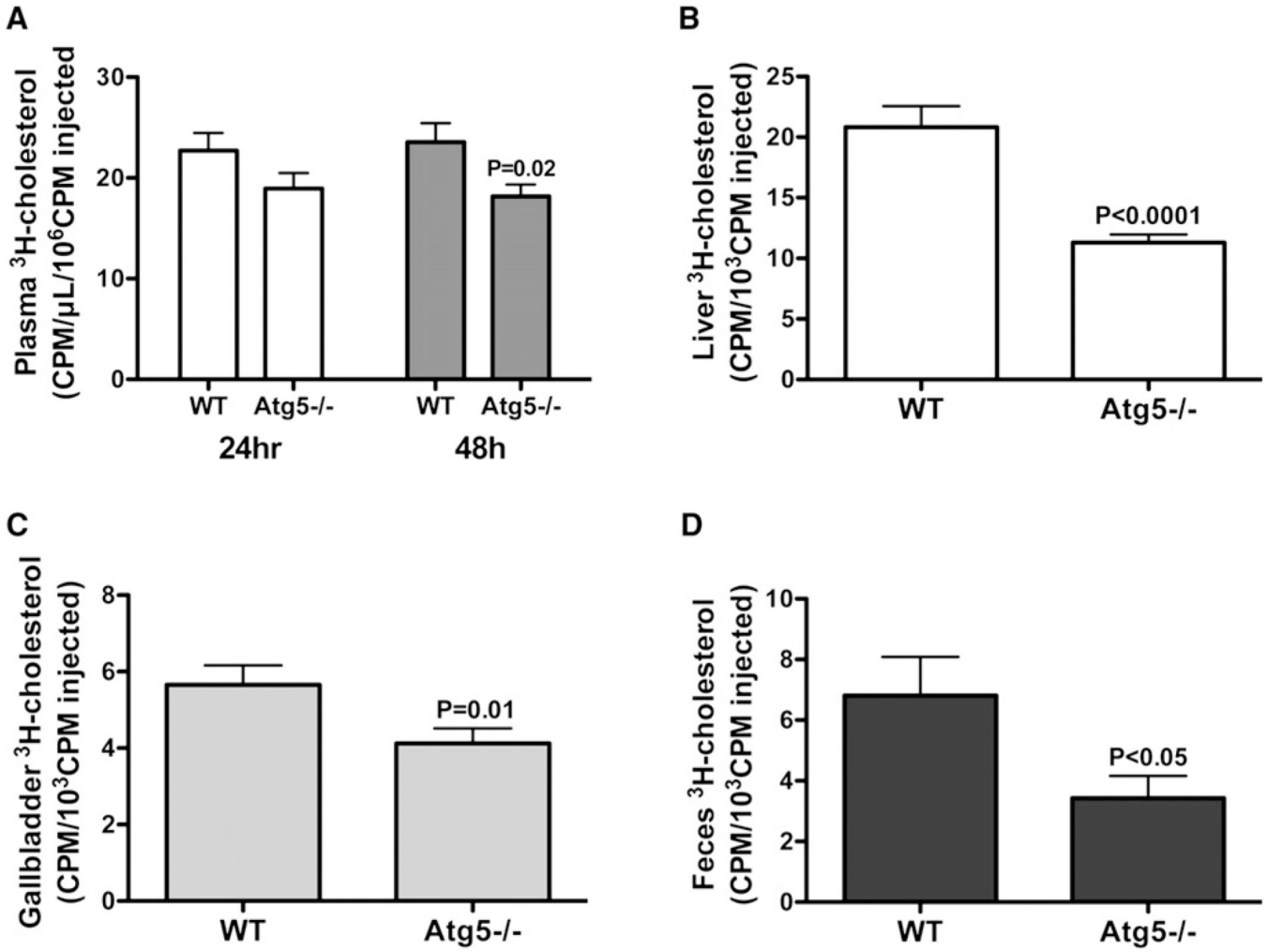

Figure 6. Macrophage-Specific Deletion of Atg5 Reduces RCT In Vivo

(A) ^{3}H-tracer in plasma at 24 and 48 hr postinjection.

(B) ^{3}H-tracer in livers at 48 hr postinjection.

(C) ^{3}H-tracer in gallbladders at 48 hr postinjection.

(D) ^{3}H-tracer in feces at 48 hr postinjection.

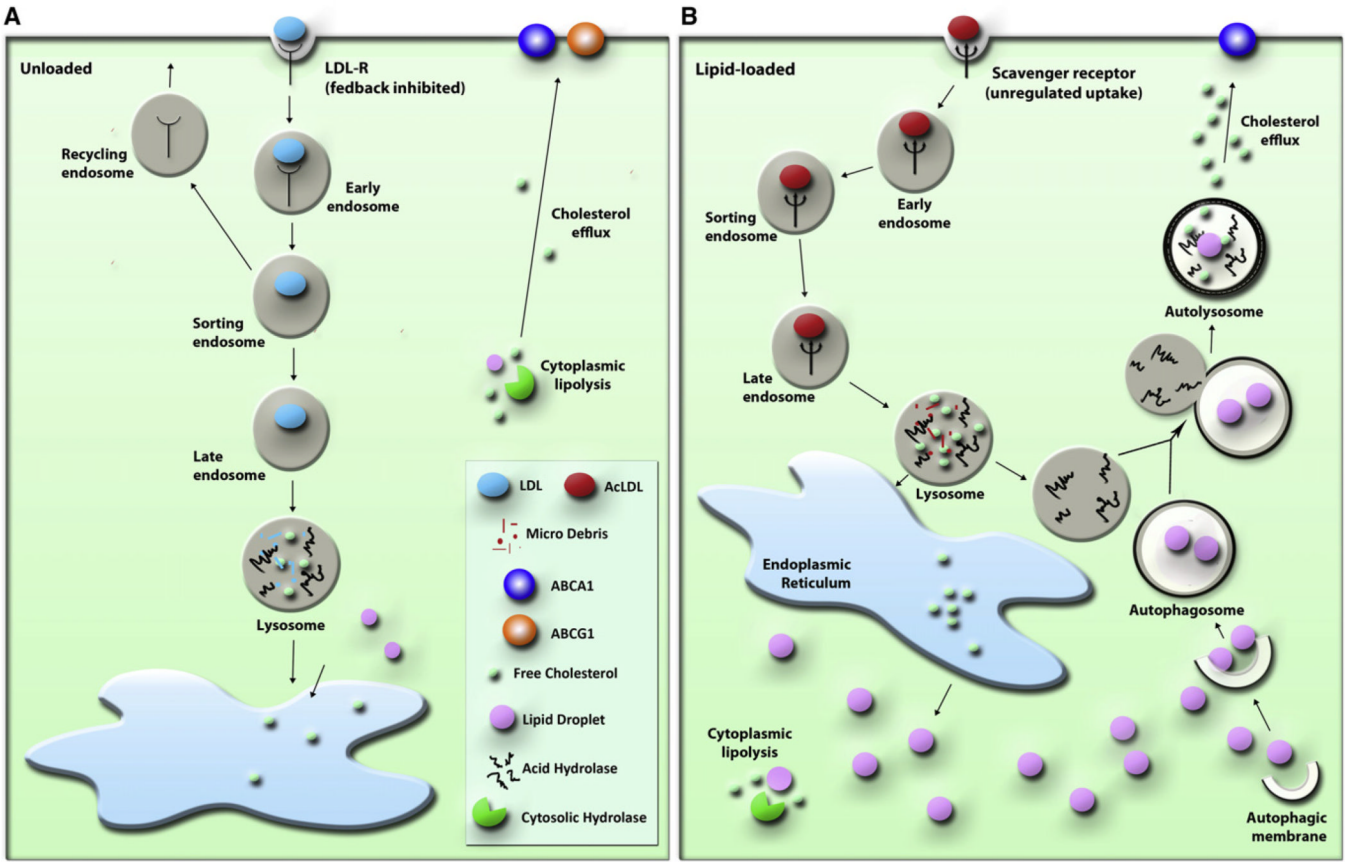

Figure 7. Model of Autophagy in LD-Associated CE Hydrolysis in Macrophage Foam Cells

(A) Cholesterol homeostasis in "normal," unloaded macrophages; a model for CE hydrolysis that mainly involves the action of neutral CE hydrolases is presented.

(B) Autophagy is induced in early macrophage foam cells, and delivery of LDs to lysosomes enhances LD-associated CE hydrolysis and cholesterol efflux.